

Evaluation of the Probable Alleviating Effect of Luteolin on Acrylamide Mediated Toxicity of the Caput Epididymal Lining Epithelium in Adult Rats: Histological and Biochemical Study

Original
Article

Iman Nabil¹, Basma A. Mady² and Amany A. Solaiman¹

¹Department of Histology and Cell Biology, ²Department of Anatomy and Embryology, Faculty of Medicine, Alexandria University, Egypt.

ABSTRACT

Introduction: Recently, acrylamide (Acr), which is a chemical compound utilised in industry, was detected in food rich in carbohydrates that had been subjected to a high temperature. It exerts its toxic effect through generation of oxidative species. Luteolin (Lut) is a potent antioxidant flavonoid that may mitigate this toxic effect.

Aim to the Work: To evaluate the histochemical changes induced by Acr on adult rat epididymal caput and the probable role of Lut in ameliorating these changes.

Materials and Methods: 30 adult rats were allocated into: group I (Control) received either distilled water (subgroup IA) or corn oil (subgroup IB), group II received 100 mg/kg/day of Lut orally, group III received 6.25 mg/kg/day of Acr orally, and group IV co-administrated Lut and Acr at doses as those of groups II and III. After 21 days, the rats were sacrificed after being weighed at the start and the end of the experiment. Sera were obtained for detection of testosterone level. Caudal fluid was collected for sperm count and motility analysis. Tissue homogenates were used to measure the level of malondialdehyde (MDA), superoxide dismutase (SOD), and the gene expression of Bcl2-Associated X Protein (BAX) and B-cell lymphoma 2 (Bcl2). Caputs were processed and examined by light and electron microscopies. All data were subjected to statistical analyses.

Results: Acr induced disruption of the caput epithelium with widening of the intercellular spaces, vacuolations, nuclear changes, reduction in sperm count and motility, a significant decline in animal weights, serum testosterone, increase in MDA and reduction in SOD. Moreover, gene expression of BAX showed a significant up-regulation with down-regulation of Bcl2. Co-administration of Lut with Acr led to improvement in structure of epididymal caput, the animal weights, the testosterone level, SOD, Bcl2, sperm count and motility.

Conclusion: Acr induced histochemical toxicity in epididymal caput, meanwhile Lut attenuated this effect.

Received: 23 June 2023, **Accepted:** 17 July 2023

Key Words: Acrylamide, epididymis, luteolin, electron microscope, sperm analysis.

Corresponding Author: Basma Mady, PhD, Department of Anatomy and Embryology, Faculty of Medicine, Alexandria University, Egypt, **Tel.** +2 010 6273 7908, **E-mail:** basma.mady@alexmed.edu.eg

ISSN: 1110-0559, Vol. 47, No. 3

INTRODUCTION

Acrylamide (Acr) is an important chemical compound which is employed in the production of water-soluble polymers involved in several industrial products like soil stabilizers, plastics, textile, paper, as well as in experimental laboratories^[1,2]. Although Acr is not a naturally occurring compound and its human exposure route was postulated to be mainly through respiration or dermal absorption, humans are now in danger of Acr exposure via its ingestion^[3]. Owing to the presence of unsaturated carbonyl group, Acr has a hydrophilic affinity and therefore it can be easily diffused throughout the body organs^[1,4].

Acr was found to be produced in many food stuff especially those rich in carbohydrates subjected to heating at more than 120°C during their preparation such as fried, baked, roasted or microwave-heated food^[5,6]. Acr is

produced as a result of the Maillard browning reaction that includes an interaction between the amino acid asparagine and reducing sugars (glucose and fructose)^[1,7]. Acr was not detected in uncooked food, consequently, it's considered as a processing contaminant^[8]. Children and young adults are at a valuable risk of Acr toxicity due to higher consumption of fried food like potato crisps^[8,9].

Acr is classified as 2A carcinogenic agent and is documented to be a genotoxin^[8], neurotoxin^[10,11], as well as a male reproductive toxin^[12,13]. The toxicity caused by Acr is attributed to its *in vivo* metabolism, where Acr is converted into its epoxide glycidamide^[14].

Acr as well as glycidamide contains the alpha and beta unsaturated amide group which can chemically react with protein nucleophiles resulting in oxidative damage of DNA, proteins and eventually the whole cells^[15].

The toxicity of Acr on the testis is very well established^[12,16-18], but little is known about its effect on the epididymis. Few research papers documented the toxic effect of Acr on epididymal spermatozoa through induction of DNA damage and alteration of the sperm small noncoding RNA profile^[19-21].

The epididymis is the site of storage as well as the functional maturation of the sperm. These functions are accomplished by the special luminal microenvironment created by the epididymal lining epithelium^[22,23].

Anatomically, the epididymis is parted into four main segments; initial, caput, corpus and cauda^[24]. The initial segment is responsible for absorption of most of the testicular fluid which accompanies the sperm during their journey. The caput and the corpus are the main sites of transformation of the immature functional sperm into mature ones which is achieved via the secretory as well as the absorptive activities of their lining epithelium. The cauda, on the other hand, serves for sperm storage before ejaculation^[25].

Regarding the lining epithelium, many cell types are identified including principal, basal, clear, halo, apical, narrow and intraepithelial migratory cells^[24]. Along the whole epididymal length, principal cells constitute the main epithelial lining cells with characteristic endocytotic and exocytotic activities^[24,26]. Functional variations of principal cells are found in different epididymal segments where caput principal cells are responsible for protein secretion that adsorbs onto sperm membrane, modifying its composition^[27].

Between the bases of the principal cells, basal cells are resting on the basal lamina^[24]. They have a protective role and may regulate the water and electrolyte transport by principal cells^[28]. Clear cells are responsible for creation of an acidic environment in the epididymal lumen in addition to their phagocytic function^[29]. Apical and narrow cells are mainly encountered in the initial segment and their functions are not yet fully understood^[24]. Halo cells and the intraepithelial migratory cells are immune cells which protect the special microenvironment of the sperm from any invasion^[29-31]. Additionally, tight junctions are created between the lining epithelium forming a blood epididymal barrier which seals the luminal microenvironment from the immune reconnaissance^[26].

Recently, a great attention has been paid towards several natural antioxidants including flavonoids, which are polyphenolic phytochemicals being abundantly present in the human diet^[32]. Flavonoids were proved in literatures to have an antioxidant effect on reproductive system in male rats^[33,34].

Luteolin (Lut 2-3,4-dihydroxyphenyl-5,7-dihydroxy-4-chromenone) is one of the natural flavones which are important subsets of flavonoids^[35]. Lut is present in almost all vegetables, fruits, leaves and natural herbs^[36]. It possesses a plethora of pharmacological properties including

antioxidant, anti-inflammatory as well as anti-apoptotic effects^[37]. Thereby, it exerts a powerful protection against organ damage including the reproductive system^[35,38].

In such a context, the present work focused on the probable toxic effect of Acr on the epididymal caput and the role of Lut in mitigating this effect.

MATERIALS AND METHODS

Chemicals

Acrylamide, luteolin (stored at 2-8°C) and corn oil were purchased from Sigma-Aldrich (St. Louis, MO, USA).

Animals

Thirty adult Wister rats (150-200 gm) were obtained from the animal house of Physiology Department, Alexandria University. The weight of each rat was measured individually and recorded at the beginning of the experiment. Temperature, humidity, and 12-hour light/dark cycles were all kept at conventional laboratory levels for the animals. All procedures were approved by the Alexandria University Faculty of Medicine's Local Medical Ethics Committee and in line with the criteria of animal care in the "Guide for the Care and Use of Laboratory Animals" IRB NO 00012098, FWA NO 00018699.

Experimental design

Four groups of rats were randomly assigned. Rats received the doses once daily via oral gavage for 21 successive days, according to the following scheme:

Group I (Control group, n=12): the rats were subdivided into two equal subgroups at random:

- Subgroup IA (n=6): each rat received 0.5 ml distilled water^[1].
- Subgroup IB (n=6): each rat received 2 mg/kg body weight corn oil^[35].

Group II (Lut group, n=6): each animal was administrated luteolin at a dose of 100 mg/kg body weight dissolved in corn oil^[35].

Group III (Acr group, n=6): each rat received a freshly prepared acrylamide solution dissolved in distilled water in a dose of 6.25 mg/kg body weight^[13].

Group IV (Lut + Acr group, n=6): the animals co-administrated Lut and Acr in the same doses as in groups II & III.

Sampling

At the end of 21 days, the rats, body weight of different experimental groups was measured and recorded. Each rat received an intramuscular injection of 70 mg/Kg ketamine combined with 7 mg/Kg xylazine^[39]. For serum testosterone measurement, blood samples were obtained from the retro-orbital venous plexus and centrifuged at 1000 x g for 15 minutes. Sera were separated and then stored at -20°C. Rats were sacrificed, the right and left epididymides

were removed, the caputs were dissected, and the right sides were processed for light microscopic examination while the left sides were cut into small pieces, some of them were taken for electron microscopic processing and the remaining pieces were stored at -80°C for further biochemical analyses. Tissue homogenates were obtained from the stored samples and were used for measurement of malondialdehyde (MDA) and superoxide dismutase (SOD) as well as for gene expression of the apoptotic marker Bcl2-Associated X Protein (BAX) and anti-apoptotic marker B-cell lymphoma 2 (Bcl2). For sperm count and motility, the caudal fluid was collected from both epididymides of each animal.

Biochemical analysis

The Biochemistry Department of the Faculty of Medicine at Alexandria University conducted all the biochemical testing.

Serum testosterone

For the quantitative measurement of serum testosterone, Enzyme-linked immunosorbent assay (ELISA) kit (Abbott, Vienna, Austria) was employed, and the results were expressed in ng/ml.

Tissue homogenate

Pieces of tissue were rinsed in a cold phosphate buffered saline (PBS) to eliminate any left blood prior to preparing the homogenate from the epididymis. Weighing the tissue pieces, soaking them in PBS (1 g tissue: 9 ml PBS), and using a glass homogenizer on ice were the next steps. The suspension was sonicated, then the supernatant was obtained by centrifuging the mixture for 5 minutes at $5000\text{ g}^{[40]}$.

MDA

The homogenate was heated at 100°C for an hour after being washed with acetic acid, sodium dodecyl sulphate, and thiobarbituric acid. After adding 5 mL of n-butanol-pyridine and 1 mL of distilled water to the prepared mixture, the mixture was vortexed. The liquid was centrifuged at 1200 g for ten minutes. The absorbance at 532 nm was measured using an ELISA plate reader (enzyme-linked immunosorbent assay)^[41].

SOD

About $100\ \mu\text{L}$ of the supernatant was incorporated with sodium pyrophosphate buffer, nitro blue tetrazolium, phenazine methosulphate, and nicotinamide adenine dinucleotide + hydrogen (NADH) to form test mixture. In order to start the reaction, NADH was used, then glacial acetic acid was added to stop the reaction. After adding n-butanol, the reaction mixture was quickly agitated. Spectrophotometer at 560 nm was used to assess the chromogen's colour intensity in butanol^[42].

Gene expression of apoptotic markers by quantitative real-time-polymerase chain reaction (qRT-PCR).

QIAzol Lysis Reagent (QIAGEN, Germany) was used to isolate total RNA from tissues. Using the commercial first-strand cDNA synthesis kit SensiFAST cDNA Synthesis kit (Meridian Bioscience, USA) and SensiFAST SYBR Green No-ROX Kit, $1\ \mu\text{g}$ of total RNA was used to produce cDNA. GAPDH gene was used as a house keeping gene. Primer sequence (Sigma Aldrich): Bcl-2 F: 5'-ATGTGTGTGGAGACCGTCAA-3' and R:5'-GCCGTACAGTTCCACAAAGGG-3'. The Bax F: 5'-ATGTTTTCTGACGGCAACTTC-3' and R: 5' AGTCCAATGTCCAGCCCAT-3'. GAPDH F: 5'-GGCACAGTCAAGGCTGAGAATG -3' and 5' R: 5'-ATGGTGGTGAAGACGCCAGTA -3'^[43].

Histological studies

1. Light microscopy (LM): the right caputs of the epididymides from all animals were fixed in 10% formol saline then processed to obtain $5\ \mu\text{m}$ thick paraffin sections stained with hematoxylin & eosin (H&E)^[44].
2. Transmission electron microscopy (TEM): pieces of the left caputs were obtained, cut into $1\ \text{mm}^3$, fixed in 3% phosphate buffer glutaraldehyde (pH 7.4) for 24 hours at 4°C and then processed to obtain semithin sections and the areas selected were examined and photographed. Further processing of the specimens was done to get ultrathin sections^[45]. Using a digital camera-equipped TEM (JEM-1400, Tokyo, Japan), electron micrographs were captured at the Faculty of Science, Alexandria University.

Sperm count and motility

For sperm count, epididymal fluid was collected from the caudas, diluted in PBS at a ratio of 1:20 ($380\ \mu\text{L}$ PBS+ $20\ \mu\text{L}$ epididymal fluid sample) and then centrifuged at 5000 rpm at 25°C for 2 minutes. $10\ \mu\text{L}$ of each diluted sample was obtained and introduced to a pre-warmed hemocytometer slide (Neubauer counting chamber). The number of sperm was counted in four large squares and multiplied by 5×10^4 ^[1,13,46].

The average sperm motility was measured in five fields as the percent of active sperm (number of active sperm to the total sperm count) multiplied by 100 ^[13,47].

Statistical analysis

Data were calculated using a statistical software application and conveyed as a mean + SD. Statistical analysis was conducted utilizing ANOVA and the post-hoc test for pair wise comparison. *P value* ≤ 0.05 was taken as a value of significance^[48].

RESULTS

No death of rats was encountered during the study.

Body weight

Compared to the weights at the beginning of the experiment, groups I (control subgroups A & B), II, III,

and IV all had significant increases in body weight (mean 189.7 ± 8.1 , 185.3 ± 9.7 , 184.7 ± 10.6 , 185.5 ± 8.2 and 185.5 ± 9.9 respectively). At the end of the experiment, no significant statistical difference was noticed between group I (A&B) and II (mean 253.7 ± 9.8 , 243.3 ± 9.7 , 241.5 ± 8.3 respectively). On the other hand, significant lower weights were recorded in group III (mean 165.2 ± 11.3) in comparison to group I and group II. Co administration of Lut and Acr in group IV (mean 209 ± 11.6) caused a significant elevation in the body weight comparing to group III, but this elevation was still significantly lower than subgroups IA, IB and group II (Figure 1).

Serum Testosterone

Significantly lower testosterone level was detected in group III (mean 0.87 ± 0.05) compared to group I (subgroup IA mean 2.22 ± 0.47 & subgroup IB mean 2.24 ± 0.50) and group II (mean 2.21 ± 0.52). Administration of Lut and Acr in group IV (mean 1.74 ± 0.43) showed significant raise in serum testosterone compared to group III. Meanwhile, the result in group IV exhibited a significant lower level in comparison to groups I and II (Figure 2).

Biochemical analysis

MDA

Significantly higher MDA level was shown in group III (mean 35.30 ± 0.51) as compared to group I (subgroup IA mean 8.60 ± 0.03 & subgroup IB mean 8.65 ± 0.03) and group II (mean 8.63 ± 0.04). In group IV (mean 14.91 ± 0.60), a significant reduction in MDA level compared to group III was detected but this level was significantly higher than groups I and II. Insignificant difference was found between groups I and II (Figure 3A).

SOD

The mean level of SOD was significantly lower in group III (mean 10.84 ± 0.56) compared to group I (subgroup IA mean 20.82 ± 0.05 & subgroup IB mean 20.78 ± 0.03) and group II (mean 20.80 ± 0.03). Concomitant administration of Lut and Acr in group IV (mean 17.33 ± 0.83) led to significant increase in SOD compared to group III. SOD level in group IV was significantly lower than groups I and II. No significant difference was detected among groups I and II (Figure 3B).

Expression of the pro- apoptotic BAX gene

Expression of BAX gene was significantly elevated in group III (mean 39.22 ± 0.31) compared to group I (subgroup IA mean 1.0 ± 0.0 & subgroup IB mean 1.0 ± 0.0) and group II (mean 0.92 ± 0.08). Providentially, co administration of Lut and Acr in group IV (mean 4.91 ± 0.02) resulted in significant reduction in the BAX gene expression compared to group III. However, the level of expression was still significantly higher in group IV than groups I and II. In comparing groups, I and II, no significant difference was noticed (Figure 4A).

Expression of the anti- apoptotic Bcl-2 gene

Significant lower expression of Bcl2 gene was shown in group III (mean 0.02 ± 0.01) compared to group I (subgroup IA mean 1.0 ± 0.0 & subgroup IB mean 1.0 ± 0.0) and group II (mean 1.0 ± 0.0). Meanwhile, significant elevation in the gene expression was detected in group IV (mean 0.48 ± 0.04) compared to the group III. On the other hand, significantly lower expression of Bcl2 gene was shown in group IV in comparison to groups I and II. Insignificant difference was found among groups I and II (Figure 4B).

Sperm count

Comparing group III (mean 6.2 ± 1.8) to group I (subgroup IA mean 87.3 ± 10.7 & subgroup IB mean 90.7 ± 12.3) and group II (mean 89 ± 7.3), the number of sperm significantly decreased in group III. Moreover, the number significantly increased in group IV (mean 51.2 ± 10) in comparison to group III. At the same time, significant lower sperm number was shown in group IV compared to groups I and II. When comparing groups, I and II, no significant difference was noticed between them (Figure 5A).

Sperm motility

The percent of motile sperm significantly declined in group III (mean 8.8 ± 1) as compared to group I (subgroup IA mean 19 ± 3.2 & subgroup IB mean 21.7 ± 3.4) and group II (mean 21 ± 2.5). While in group IV (mean 14.3 ± 1.6), the percent was significantly higher than in group III, but still significantly lower than in groups I and II. The motile sperm percent in group I showed insignificant difference compared to group II (Figure 5B).

Light microscopic examination

a-Haematoxylin and eosin stains (H&E)

Group I (Control group): The control rat epididymal caput (subgroups IA & IB) revealed multiple transverse sections of the ductus epididymis that were separated by scanty connective tissue. Each one was lined by pseudo-stratified columnar epithelium with stereocilia and showed average content of sperm within the lumen.

Principal cells were closely arranged and extended from the basal lamina towards the lumen. They were topped with numerous and extremely long stereocilia. They showed spherical, pale and basally situated nuclei.

Between the basal portions of the principal cells, basal cells were dispersed and lying on the basal lamina. They exhibited horizontally-placed oval nuclei that were surrounded by scanty amount of cytoplasm. Apical cells with apically located nuclei were also encountered between the principal cells. Few halo cells were shown. They were characterized by being small and rounded in shape, contained spherical and central nuclei surrounded by a clear rim of cytoplasm (Figure 6A,B).

Group II (Lut group): This group's rat epididymal caput demonstrated the same histological structure as the control group. (Figure 6C).

Group III (Acr group): Histological examination revealed many structural changes. The intertubular spaces were widened with increase in the amount of connective tissue in between. The lumina of some tubules exhibited scanty amounts or even absence of sperm, others contained cell debris. The lining epithelium was disrupted. The apical surface of the lining cells revealed few stereocilia that was even nearly lost in some areas. Widening of the intercellular spaces and separation of the epithelial cells from the basal lamina were depicted. Multiple cells showed deeply stained nuclei. Cytoplasmic vacuolization was noticed in some cells. Many halo and clear cells were encountered (Figure 7A-D).

Group IV (Lut + Acr group): The rat epididymal caput revealed apparently normal tubules. Few sperm appear in the lumina of some tubules while they are absent in the others. They further revealed apparently normal lining cells except for few principal cells with karyolysis and some other cells with cytoplasmic vacuolations. Many halo cells are still frequently encountered (Figure 8).

b- Toluidine blue stain

Examination of semithin sections of the ductus epididymis in group I & II revealed the pseudostratified columnar epithelium with long stereocilia with their characteristic shapes and location. Group III that received Acr showed wide intercellular spaces and cellular vacuolations. Clear cells were frequently encountered. They were characterized by their pale and vacuolated cytoplasm. Sloughed cells within the lumen were frequently encountered. Group IV which received Lut with Acr showed a normally apparent histological structure of the lining epithelium (Figure 9A-F).

Electron microscopic examination

Group I (Control group): The caput showed lumina lined by well-defined pseudostratified columnar epithelial cells with stereocilia. Principal, basal, clear and halo cells constituted the lining epithelium.

Principal cells appeared tall columnar having spherical and euchromatic nuclei with prominent nucleoli. The apical free borders had stereocilia. Their apical cytoplasm contained numerous lysosomes. In the supranuclear region, multiple well-developed Golgi stacks were shown. Basally, parallel cisternae of rough endoplasmic reticulum and mitochondria were noticed.

Basal cells were triangular and were observed to be in intimate contact with the basal lamina between the basal parts of the principal cells. Their oval, euchromatic nuclei were located horizontally.

Halo cells appeared rounded and were located at different levels. They were characterized by large,

spherical, and central nuclei contained within a scanty clear electro-lucent cytoplasm.

Clear cells were infrequently encountered, interspersed among principal cells. They were distinguished by abundant large vacuoles in their cytoplasm. They further had euchromatic nuclei and lysosomes as well as few microplicae projecting from their apical membranes. Blood epididymal barrier was depicted between adjacent epithelial cells of the epididymis (Figure 10A-F).

Group II (Lut group): Caput epididymis from luteolin treated animals showed normal architecture as in the control group. (Figure 11A-C).

Group III (Acr group): Histopathological alterations were observed in the lining epithelium of the epididymal caput. The intercellular spaces were widened between the principal cells and the basal cells, the latter were partially detached from the basal lamina. Nuclear degenerative changes were seen in some nuclei of the principal cells; some nuclei appeared heterochromatic and irregular in outline, others were shrunken with disintegrated chromatin. Marginated nucleoli were evident in some cells. Some principal cells revealed marked cytoplasmic vacuolation as well as dilated profiles of rough endoplasmic reticulum. Halo cells appeared more frequently, some of them showed cytoplasmic vacuolations. Sloughed cells were observed within the lumen. Blood epididymal barrier was observed (Figure 12A-F).

Group IV (Lut+Acr group): Examination of the rat epididymal caput displayed closely opposed cells with a prominent blood epididymal barrier. The nuclei of principal cells were basally located and appeared euchromatic, nearly like the control. Meanwhile, some cells revealed vacuolations and dilated profiles of the rough endoplasmic reticulum while others depicted shrunken nuclei with peripheral clumping of disintegrated chromatin (Figure 13A-D).

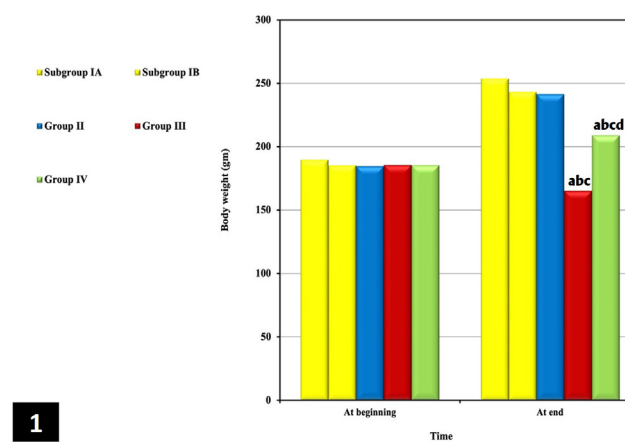


Fig. 1: Comparison of the body weights of the various studied groups at the beginning and at the end of the experiment (a,b,c&d; significance with subgroups IA, IB, groups II, III&IV respectively)

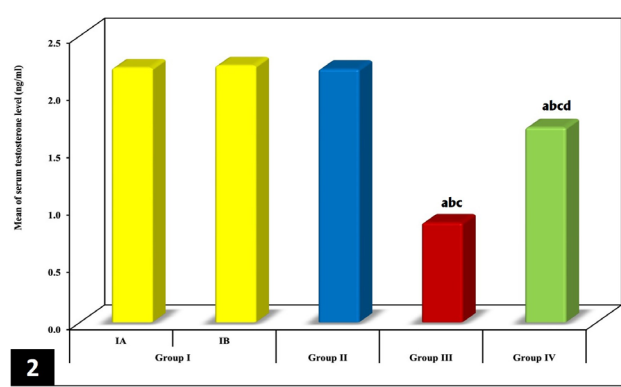


Fig. 2: Comparison of the levels of serum testosterone in the different studied groups

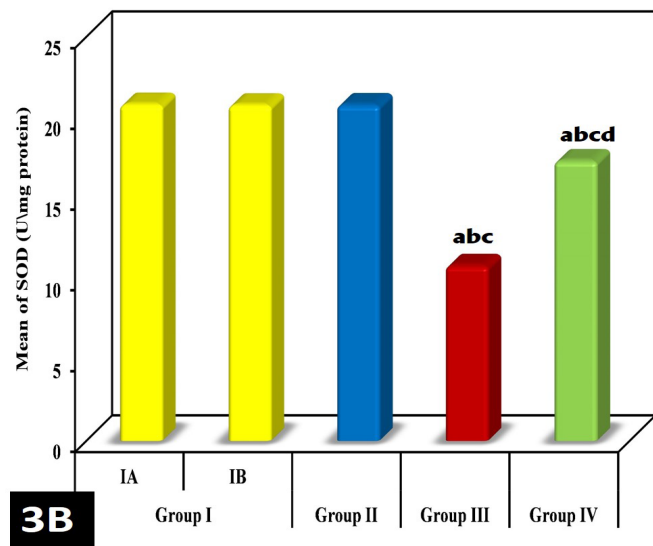
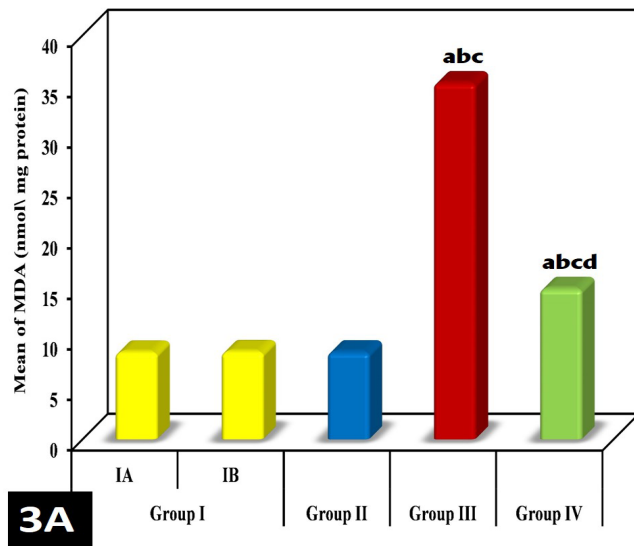


Fig. 3A,B: Comparison of the various experimental groups based on the tissue levels of A) MDA and B) SOD

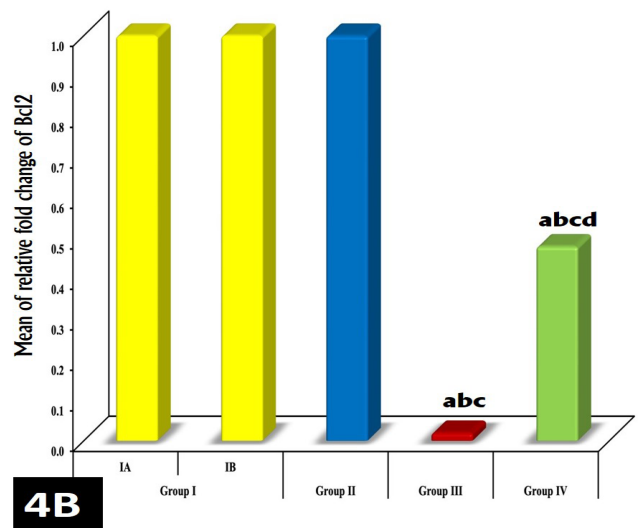
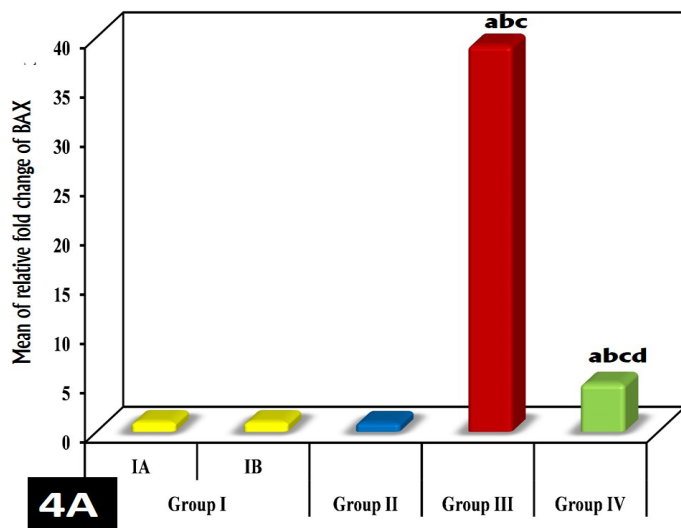


Fig. 4A,B: Comparison of the various experimental groups based on the relative fold change in A) BAX and B) Bcl2 gene expression

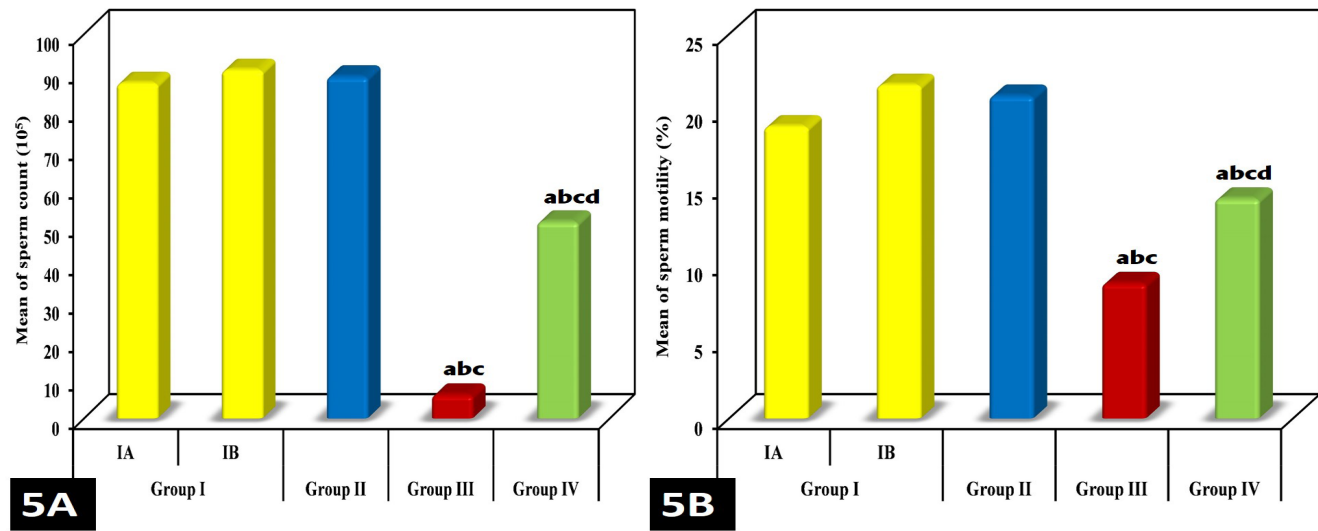


Fig. 5A,B: Comparison of the various experimental groups based on A) Sperm count and B) Percent of sperm motility

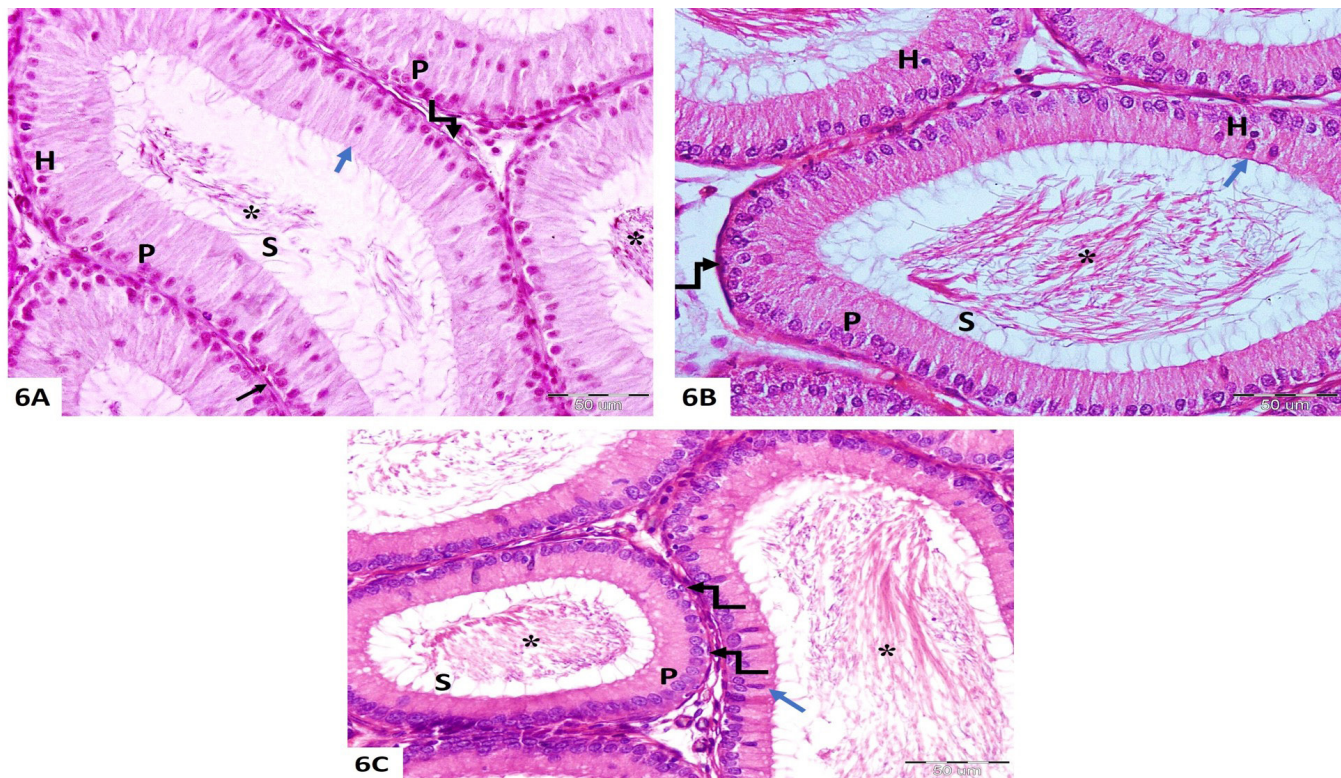


Fig. 6A-C: Photomicrographs of rat epididymal caput: A) Subgroup IA (control group received distilled water), B) Subgroup IB (control group received corn oil) and C) Group II (Lut group). Multiple transverse tubules of the ductus epididymis are seen separated by minimum amount of connective tissue, each tubule is lined by pseudostratified columnar epithelium with stereocilia. The epithelial lining consists mainly of tall columnar principal cells (P) that contact the basal lamina and their luminal surface carries apical stereocilia (S), their nuclei are spherical and generally occupies the lower third of the cytoplasm. Basal cells (elbow arrow) are small triangular cells with a small amount of cytoplasm and horizontally oval nucleus, they lie on the basal lamina but don't reach the lumen. Goblet-shaped like apical cells (blue arrow) with an apical nucleus are also encountered. Halo cells (H) appear small and rounded with small and spherical nuclei surrounded by a pale cytoplasm in A and B. Multiple sperm (*) are observed within the ductus lumen. H&E stain, Mic.Mag. X 400

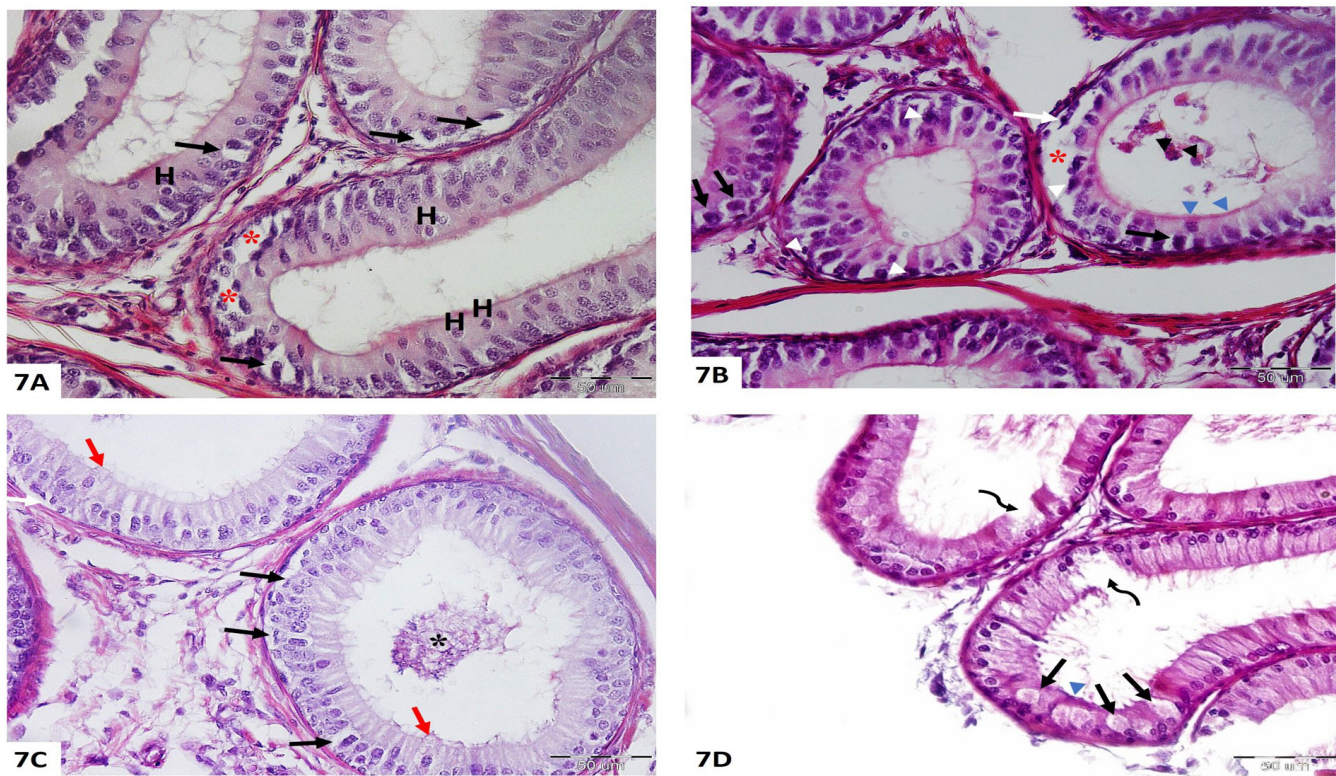


Fig. 7A-D: Photomicrographs of group III rat epididymal caput (Acr group) reveals: A) Distorted epithelial cells with wide intercellular spaces (red*) and vacuoles (↑), multiple halo cells (H) are encountered. No sperm are detected in the lumina. B&C) Disruption of the lining epithelium with separation of the lining cells from the basal lamina (white↑) and vacuolations (black↑). In B, wide intercellular spaces (red*), cell debris within the lumen (black ^), short or even lost stereocilia (blue ^) and lining cells with dark nuclei (white ^) are observed. In C, clear cells with apical vacuolated cytoplasm (red ↑) and sperm within the lumen (black*) are seen. Notice: widening of the intertubular spaces in B&C with increase in the connective tissue stroma in C. D) Disruption of the lining epithelium (curved arrow), multiple clear cells (↑) with shortening or even loss of the stereocilia (blue^). H&E stain, Mic.Mag. X 400

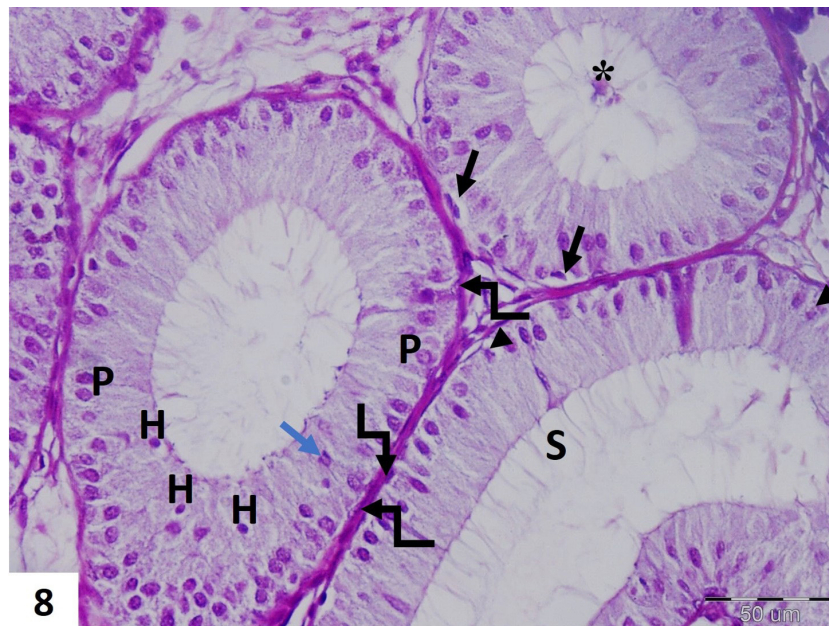


Fig. 8: Photomicrograph of rat epididymal caput (group IV; Lut+Acr group) shows apparently normal lining epithelium with principal cells (P), basal cells (elbow arrow), apical cells (blue arrow) and many halo cells (H). Few principal cells depict karyolysis (^). Some vacuolations (↑) are still encountered within the lining cells. H&E stain, Mic.Mag. X 400

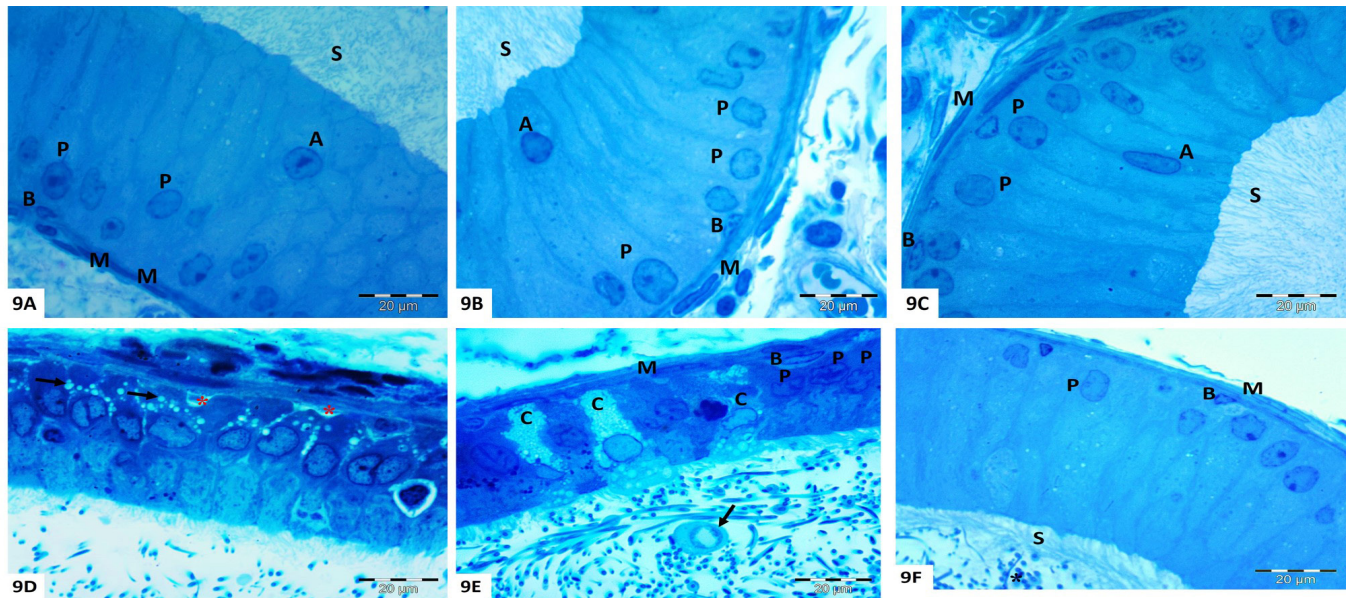


Fig. 9A-F: Photomicrographs of semithin sections of the epididymal caput: A) Control subgroup IA, B) Control subgroup IB and C) Group II (Lut group) reveal the pseudostratified columnar epithelium with long stereocilia. Tall columnar principal cells (P) with a spherical and generally basal nuclei are the main lining cells that extend from the basal lamina toward the lumen with their characteristic long stereocilia (S). Basal cells (B) are small triangular cells with a horizontally oval nucleus, are seen resting on the basal lamina but don't reach the lumen. Apical cells (A) with a rounded and apical nucleus, the cells don't apparently contact the basal lamina but reach the lumen. M; smooth muscle cells. D) Group III (Acr group) reveals wide intercellular spaces (red*) and multiple vacuoles (†). E) The same group shows abundance of clear cells (C) which are large cells with pale cytoplasm that contain numerous vacuoles. Sloughed cell (†) with a degenerating nucleus is seen within the lumen. F) Group IV (Lut+Acr group) depicts normally appearing lining epithelial cells with principal cells (P) and basal cells (B), black*; sperm in the lumen. Toulidine blue stain, Mic.Mag. X 1000

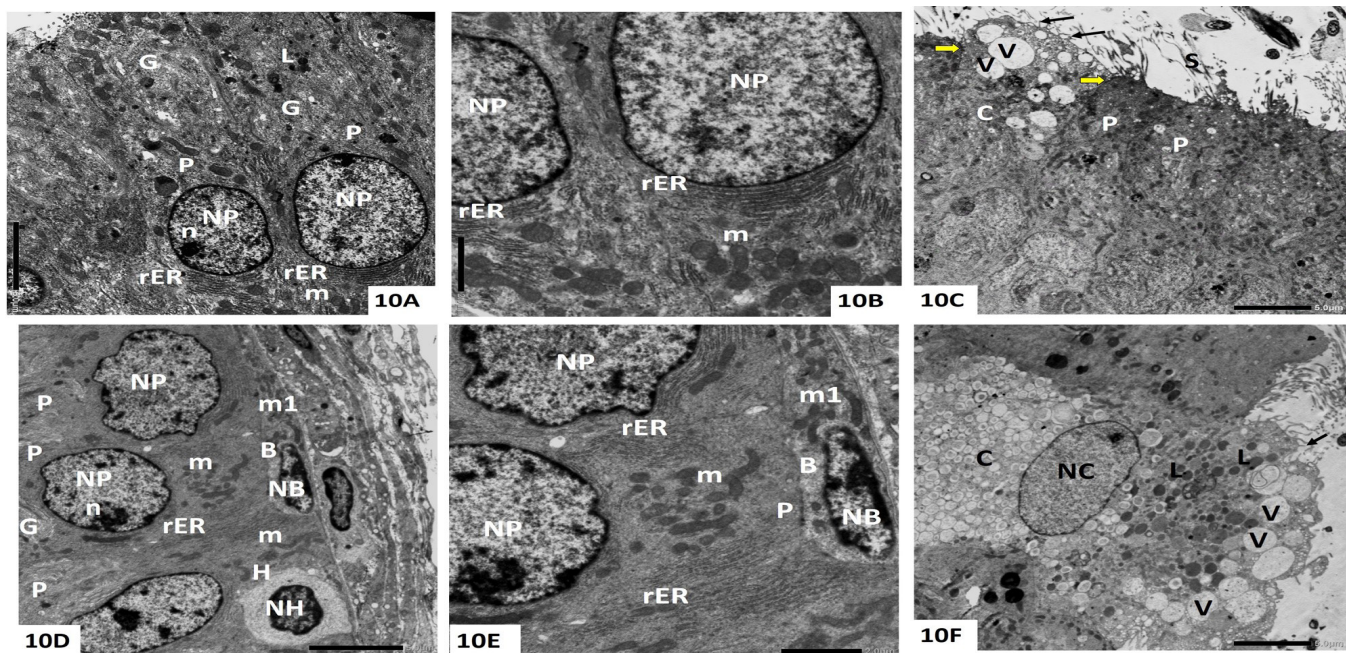


Fig. 10A-F: Electron microscopic pictures of a control rat epididymal caput (group I), A-C: subgroup IA, D-F: subgroup IB) show: A&B) Principal cells (P) with a spherical and euchromatic nucleus (NP) with a prominent nucleolus (n), a large supranuclear Golgi apparatus (G), lysosomes (L), many mitochondria (m) and basal parallel cisternae of rough endoplasmic reticulum (rER). C) A clear cell with micropliae (†) projecting from its luminal border and a cytoplasm with many vacuoles (V). S; stereocilia, thick yellow arrow; blood epididymal barrier. D&E) A part of the lining epithelium of the epididymis reveals principal cells (P) with well-developed supranuclear Golgi cisternae (G), numerous parallel arrays of the rER occupy the basal portion of the principal cells with numerous mitochondria (m), a small triangular basal cell (B) rests on the basal lamina with a horizontally oval and euchromatic nucleus (NB) surrounded by a scanty electrolucent cytoplasm, m1; mitochondria in the basal cell. A halo cell (H) in D with a large and spherical nucleus (NH) that depicts peripheral condensation of the heterochromatin and surrounded with an electrolucent cytoplasm. F) A clear cell (C) shows an euchromatic nucleus (NC) and a cytoplasm filled with numerous vacuoles (V) of variable electron densities and few lysosomes (L). †; micropliae. Uranyl acetate and lead citrate, Mic. Mag. A&Dx1500, B&Ex3000, C&Fx1200

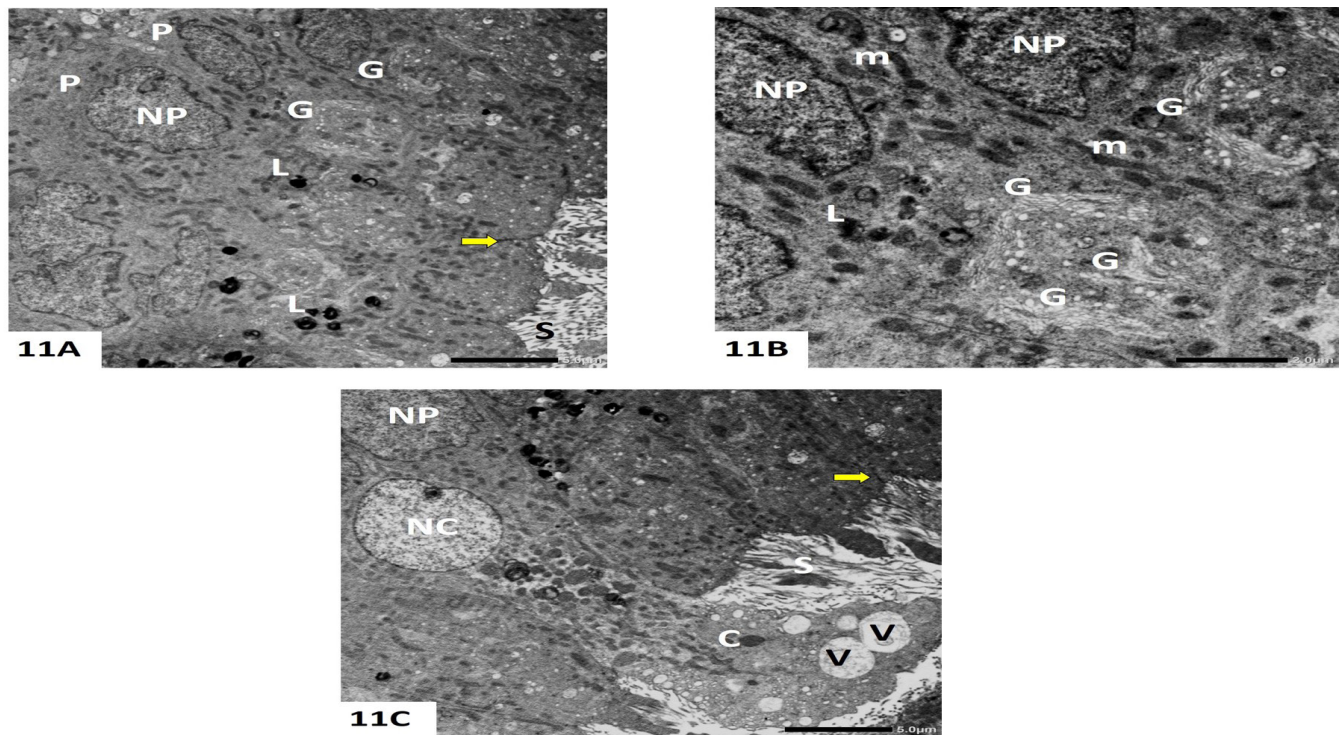


Fig. 11A-C: Electron microscopic pictures of rat epididymal caput (group II; Lut group): A&B) Principal cells (P) with a spherical and euchromatic nucleus (NP), many supranuclear Golgi stacks (G), mitochondria (m) and multiple apical lysosomes (L), S; stereocilia. C) A clear cell (C) with a rounded and euchromatic nucleus (NC) and vacuoles of variable electron densities (V). In A&C: blood epididymal barrier (thick yellow arrow). Uranyl acetate and lead citrate, Mic. Mag. A&Cx1200,Bx3000

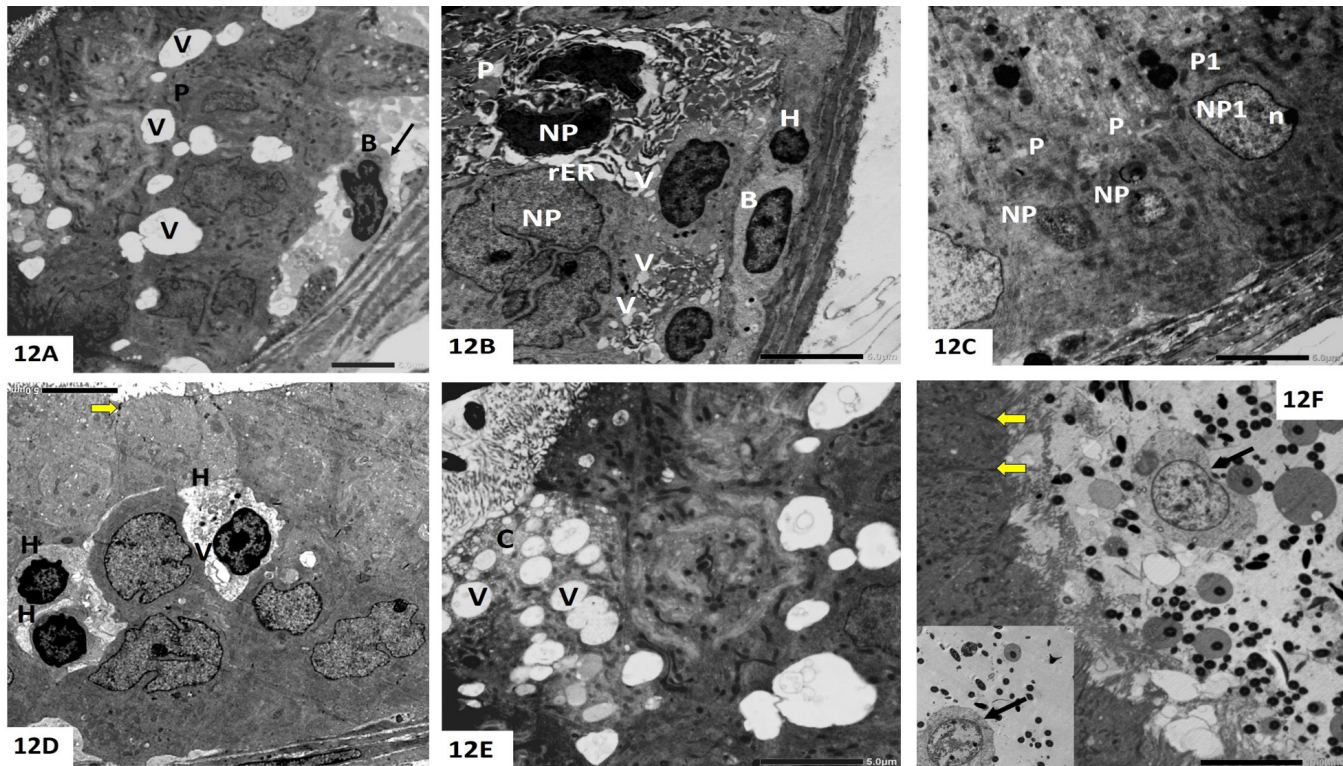


Fig. 12A-F: Electron microscopic pictures of a group III rat epididymal caput (Acr group). A) A wide intercellular space (↑) with a partially detached basal cell (B) from the basal lamina, a vacuolar degeneration (V) within the cytoplasm of the principal cells. B) A principal cell (P) with a heterochromatic and a highly irregular nucleus (NP), dilated rER and multiple cellular vacuolations (V) are encountered, H; a halo cell, B; a basal cell. C) Principal cells (P) with a shrunken nucleus (NP) contain disintegrated chromatin, another principal cell (P1) had a nucleus (NP1) with a marginated nucleolus (n). D) Numerous halo cells (H) are encountered with cytoplasmic vacuolations (V). E) A clear cell (C) with multiple vacuoles (V). F) Sloughed cells (↑) within the lumen of the epididymis, one shows a nucleus with disintegrated chromatin (inset). In D&F: blood epididymal barrier (thick yellow arrow). Uranyl acetate and lead citrate, Mic. Mag. Ax1000, B,C&Ex1500, D& insetx1200, Fx800

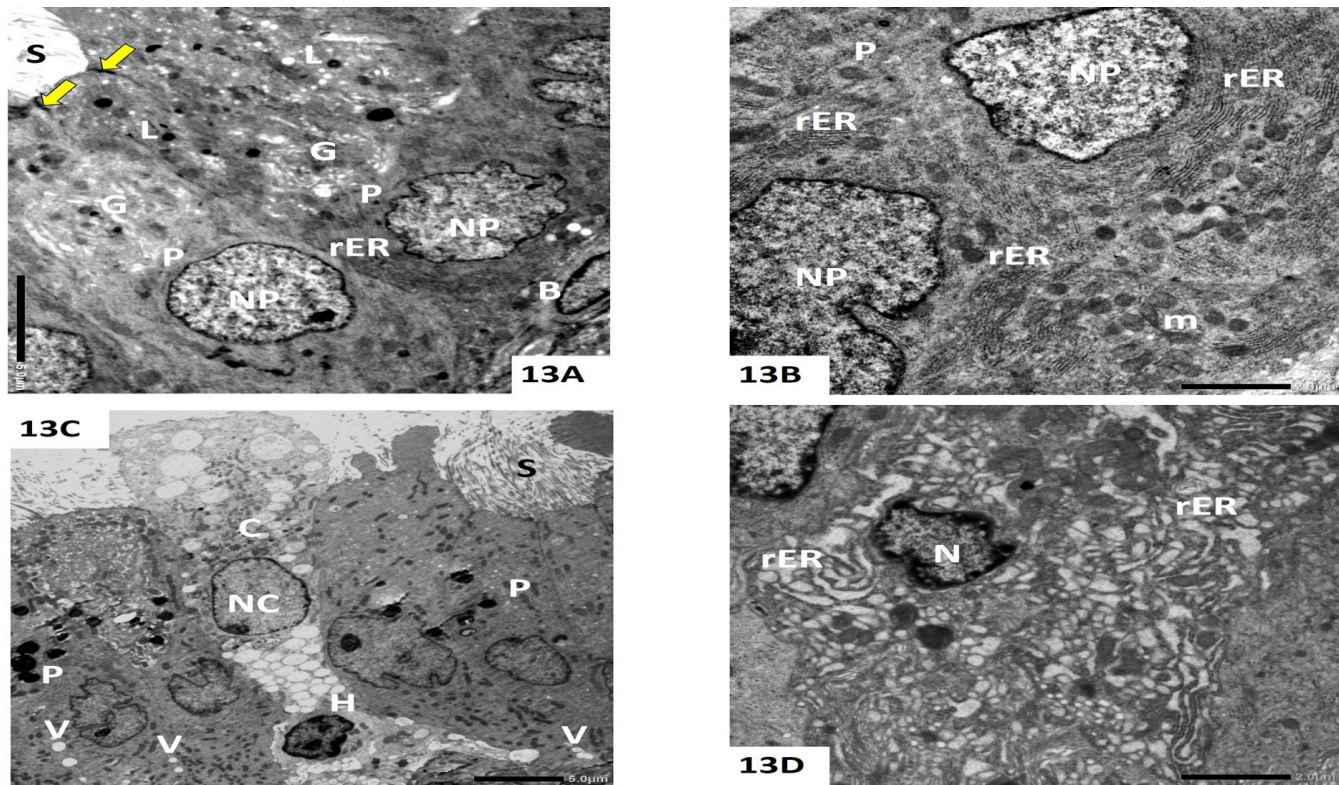


Fig. 13A-E: Electron microscopic pictures of rat epididymal caput (group IV; Lut+Acr group). A) Principal cells (P) with a spherical and euchromatic nucleus (NP), a large supranuclear Golgi apparatus (G), lysosomes (L) and multiple basal profiles of rER, B; part of a basal cell. Thick yellow arrow; blood epididymal barrier. B) A high magnification shows multiples parallel arrays of rER and many mitochondria (m) within the principal cells' cytoplasm. C) A clear cell (C) and a halo cell (H) are apparently normal, some vacuoles (V) are encountered within the principal cells' cytoplasm (P). D) Another principal cell shows shrunken nucleus (N) with peripheral clumps of disintegrated chromatin together with a prominent dilated rER. Uranyl acetate and lead citrate, Mic. Mag. Ax1500, B&Dx3000, Cx1000

DISCUSSION

Subfertility and infertility constitute major health problems affecting millions of couples at reproductive age around the world with male reproductive disorders accounting for more than 30% of the causes of infertility^[49,50]. The recent high incidence of infertility suggests environmental exposure to certain chemicals especially in food constituents^[51]. Nowadays, many components of food were known to cause toxic effects on gonads in male rats as well as disruption of the endocrine system, subsequently affecting their reproductivity^[50].

Many years ago, Acr toxicity had been raised among industrial workers especially during manufacturing paper, cosmetics and polyacrylamide gel^[52]. However, Acr was recently detected in food products subjected to high temperature especially carbohydrate rich food, accordingly human exposure to Acr becomes progressively booming^[5,12].

Acr is an intermediate product produced as a consequence of condensation reactions during thermal processing of food^[4]. The metabolites of Acr include N-acetyl- S- cysteine, glyceramide and glycidamide, the latter is the key factor responsible for Acr-induced toxicity as a consequence of formation of glycidamide-DNA and thiol groups adducts^[7,8,53]. Evidence from several

studies addressed the detrimental effects of Acr on many organs including the reproductive system of rats and mice^[1,5,7,10-12,50].

While most of the previous investigators devoted to illustrating the toxic effect of Acr on the testis^[1,5,7,12,50], little is known regarding its effect on the epididymis. As opposed to the testis which harbour the sperm development, the epididymis has a vital task in functional maturation of the spermatozoa^[22].

Noteworthy, Katen *et al.*^[19] reported a selective impact of Acr on the epididymis which was ascribed to cytochrome P450 2E1; an enzyme that is responsible for Acr metabolism, is found to be highly expressed in the lining epithelium of the epididymal caput, in turn this enzyme converts Acr to its toxic metabolite glycidamide.

Moreover, it was postulated that after few hours of oral administration, Acr distributes easily throughout the body organs reaching the testis and the epididymis where it is converted in the latter by the epididymal epithelium into glycidamide^[19]. Even though the epididymal-blood barrier is found between the principal cells especially in the caput region to protect the spermatozoa microenvironment from blood-borne toxins^[54], glycidamide can cross this barrier owing to its small molecular weight and its hydrophilic nature, reaching the epididymal lumen where

the spermatozoa are stored, adducts with their DNA and eventually induces DNA damage^[19].

In the same context, the results of this work suggested detrimental effects of Acr on the epididymis of adult male rats in group III which were shown generally by a significant reduction in the body weight, and specifically on the epididymal tissue via a significant elevation in epididymal oxidative stress and apoptotic markers concomitant with a significant decline in the antioxidant enzymes and anti-apoptotic protein expression compared to the other three experimental groups. These biochemical changes coincided with a significant alteration in sperm parameters as well as structural damages of the epididymal caput.

On measuring the body weight at the beginning and at the end of the current experiment, a significant reduction in the body weight was noticed in Acr-treated rats in comparison to the other experimental groups. In general, loss of body weight is considered as one of the forerunners indicating the non-specific toxicity induced by Acr^[13].

It was well established that oxidative stress and overproduction of reactive oxidant species (ROS) play their roles in Acr toxicity. Indeed, Acr and its toxic metabolite glycidamide disrupt the balance between the oxidants and the antioxidants within the cell leading to release of lipid peroxides such as MDA that destroy the lipid matrix in the membranes^[55]. At the same time, Acr reduces the activity of antioxidant enzymes that are considered as the first line of defence against ROS and their toxic compounds such as hydrogen peroxide, hydroxyl radical and superoxide anion^[11,12,55,56]. Consequently, loss of mitochondrial membrane potential, dysregulation of proapoptotic and antiapoptotic proteins, release of cytochrome-C and activation of caspase 3 reactions results ultimately in cell apoptosis^[11,56].

In consistent with previous research works^[5,16,56,57], the results of the present work displayed a disturbance in the oxidant and antioxidant power of the epididymal tissue treated with Acr which was manifested by a significant elevation in the tissue MDA level accompanied by a significant reduction in SOD compared to the other three experimental groups. Moreover, a significant up-regulation in the pro-apoptotic BAX gene expression as well as a significant down-regulation in the expression of the anti-apoptotic gene; Bcl2 was noticed in this group reflecting the apoptotic effect of Acr on epididymal tissue. Studies on Acr attributed its lethal effect on the cells to an increase in BAX/ Bcl-2 ratio owing to intracellular accumulation of ROS as well as inflammatory cytokines which eventually induce the cell for programming its death^[7,56-59].

As a consequence of a deficiency of an effective endogenous antioxidant protective mechanism against reactive oxidants and a deprivation of the supportive microenvironment exerted by Sertoli cells, the epididymal spermatozoa are more prone to the injurious effects induced by ROS^[60]. In addition, the spermatozoa cell

membrane is more vulnerable to the effect of ROS owing to its high content of polyunsaturated fatty acids, which disrupt the membrane fluidity resulting in disturbance of the sperm motility^[61]. Hence, the current work recorded a dramatic fall in the sperm count and motility in Acr-treated group. Yang *et al.*^[62] explained this reduction by the direct toxic effect of lipid peroxides on the sperm membrane. Moreover, Trigg *et al.*^[20] declared that Acr can induce DNA damage and change in the small RNA profiles of the epididymal spermatozoa, thereby gene expression dysregulation occurred. Furthermore, the significant reduction in the sperm motility in Acr group could be also explained by its direct toxic effect on kinesin motor protein which is present in sperm flagella^[63,64].

Meanwhile, testosterone is a vital hormone orchestrating the process of spermatogenesis^[65]. Therefore, a disruption in its level adding another negative impact on the sperm parameters^[5,57,64]. Testosterone deprivation leads to diminution in the normal number of sperm travelling to the epididymis. In addition, the epididymis is an androgen-dependant organ, which relies on testosterone to maintain its normal structure and function, subsequently, deficiency of testosterone disrupts the epididymal epithelium, consequently lessens the androgen-dependant phases of sperm maturation^[27].

In the current work, estimation of the serum testosterone level in group III rats exposed to Acr showed a substantial decline in comparison to the other three experimental groups. This result was in consistent with earlier research which reported a dose-dependent decline in serum testosterone caused by Acr^[5,12,16,62,66]. It was documented that Acr disrupts the serum testosterone by either a direct lethality on Leydig cell or indirectly via hepatic conversion of testosterone into metabolic products of lower androgen binding activity^[67,68].

The deleterious effects of Acr on the structures of many body organs were previously reported but few literatures discussed its histopathology detected by the light microscopy on the epididymal tissue and so far, no literature pronounced its effect on the ultrastructure level. In the present study, examination of rat epididymal caput by the light microscope in the group administrated Acr (group III) revealed pronounced structural changes including loss of stereocilia, vacuolation, pyknotic nuclei as well as widening of the intercellular spaces and separation of the lining epithelium from the basal lamina. The lumina appeared either empty or containing cell debris.

Similarly, Kalaivani *et al.*^[13] declared degenerative vacuolar changes of the testis and epididymis following Acr administration. Moreover, Lebda *et al.*^[17] demonstrated sloughed epithelial cells with low number or even absent spermatozoa in the epididymal lumina, oedema as well as interstitial mononuclear cellular infiltration in Acr treated rats. Furthermore, Ma *et al.*^[66] illustrated the toxicity of Acr on the epididymis as manifested by reduction in the luminal sperm, disarrangement and degeneration of the epithelial cells.

The light microscopic findings were further confirmed by the electron microscopy in the current work which revealed marked nuclear and cytoplasmic degenerative changes affecting mainly the principal and basal cells in the caput in group III. These changes included shrunken, heterochromatic, and irregular nuclei with chromatin disintegration, cytoplasmic vacuolation and dilated endoplasmic reticulum. These histological changes could be attributed partially to the ability of ROS to combine with different cellular molecules including membrane lipids, proteins and nucleic acids, resulting in alteration in the membrane permeability and integrity, DNA fragmentation together with change in the mitochondrial membrane with subsequent release of cytochrome C into the cytoplasm triggering apoptosis of the cells^[61]. In addition, testosterone deficiency as well might share in the observed structural changes in the epididymal caput in rats received Acr. Such alterations in the normal structure of the caput epithelium definitely disrupt the function of the lining cells, accordingly alter the composition of the luminal fluid and eventually interrupt the luminal sperm themselves^[27].

Moreover, a remarkable feature in rats exposed to Acr, was frequently encountered clear cells. This finding was also reported by Mohamed *et al.*^[69] on studying the effect of cigarette smoke on rats epididymis. It was known that clear cells are responsible for phagocytosis of sperm residual droplets and participate in acidification of the intraluminal fluid^[29]. De Andrade *et al.*^[70] correlated between the increase in the number and size of clear cells and the decrease in the cauda sperm density that they noticed in rats after exposure to gossypol. Simply, clear cells responded to the increase in their functional demand by undergoing hyperplasia and hypertrophy in an attempt to remove the degenerated and the abnormal sperm^[66].

Additionally, many halo cells were noticed in Acr treated group. Halo cells are intracellular lymphocytes that are present along the whole length of the epididymis. They have a fundamental role in the immunological barrier of this organ. Their increase in number in the epididymal lining cells after Acr exposure could be a sign of immune response due to release of inflammatory mediators as NF- κ B, TNF- α , IL-6, IL-1 β and COX-2^[71].

Nowadays, the naturally existing compounds have been extensively investigated for management of many diseases. Luteolin (Lut) is a natural flavonoid found especially in citrus fruits and vegetables^[32].

Co-administration of Lut and Acr in the present work in group IV mitigated the toxic effects elicited by Acr on epididymal caput in rats by improving the body weight gain as well as the redox status of the cells and lessening the mitochondrial-mediated apoptosis. In addition, the administration of Lut obviously moderated Acr-induced alteration in serum testosterone, sperm parameters and the epididymal caput histology. Therefore, in comparison to group III which received Acr alone, concomitant

administration of Lut and Acr led to significantly higher body weight gain, SOD level, Bcl2 expression, sperm parameters and serum testosterone. Meanwhile, Lut with Acr caused significant reduction in MDA level and BAX expression as well as apparent preservation of the histologic structure apart from persisting degenerative foci existed in few principal cells. These findings coincided with other studies stating that Lut can abate the reproductive disruption induced by many toxic compounds^[35,72] owing to its antioxidant^[35,73,74], anti-inflammatory^[35], and anti-apoptotic effects^[35,75].

In consistent with our results, Owumi *et al.*^[35] reported the abating effect of Lut against doxorubicin-induced testicular and epididymal damage. They found that Lut significantly restored the body weight and serum testosterone of rats, decreased the level of MDA with concomitant increase in SOD, down-regulated BAX expression accompanied with up-regulation of Bcl2 as well as improved the normal architecture of the testis and epididymis. They attributed the ameliorative effect of Lut to its ability to scavenge ROS, reduce proapoptotic proteins and lessen inflammatory cytokines.

Many previous research studies elucidated the protective role of Lut by exerting a combined action of ROS scavenging ability and anti-apoptotic inhibiting effect via suppression of apoptotic inducers such as BAX, MAPK and p38, in addition to activating the expression of many other genes silenced the apoptosis as Bcl2, Keap1, and Nrf2^[73,75-77].

Nrf2 (The nuclear factor erythroid 2-related factor 2) is a pivotal controller of cellular resistance whenever oxidative stress fulminates^[78]. It regulates the expression of antioxidant-related genes to overcome the surge in ROS level. Uncontrolled production of oxidant markers activates Nrf2 which moves from the cytoplasm to the nucleus, binds to several genes, in turn regulates plethora of reactions including antioxidant production, inflammatory signals, autophagy, mitochondrial biogenesis and apoptosis^[78,79].

Exposure to Acr has been linked to Nrf2 pathway. Nevertheless, controversial results have been obtained about the decrease or the increase in Nrf2 level during exposure to Acr. However, the majority of the studies reported an activation of Nrf2 following Acr administration in attempt to overcome the uncontrolled production of ROS^[58]. Furthermore, the use of antioxidants enhances this natural protective effect via augmentation of the expression of Nrf2 with subsequent alleviation of the toxicity induced by Acr^[58,80].

In this context, many researchers delineated that Lut activated Nrf2 signalling pathway, boosting its nuclear translocation, increasing the expression of antioxidant genes, decreasing ROS, inhibiting apoptosis, and eventually improving the cellular activities^[74,81].

Thus, the current study emphasized the attenuating effect of Lut against Acr-elicited toxicity on epididymal

caput at hormonal, biochemical and structural levels. So far, this work was the first to describe the effect of Acr and Lut on the epididymis at the ultrastructure level.

CONFLICT OF INTERETS

There are no conflicts of interest.

REFERENCES

- Ahmed MM, Hammad AA, Orabi SH, Elbaz HT, Elweza AE, Tahoun EA, *et al.* Reproductive injury in male rats from acrylamide toxicity and potential protection by earthworm Methanolic extract. *Animals*. 2022;12(13):1723.
- Tepe Y, Çebi A. Acrylamide in environmental water: a review on sources, exposure, and public health risks. *Expo Health*. 2019;11:3-12.
- Pedersen M, Vryonidis E, Joensen A, Törnqvist M. Hemoglobin adducts of acrylamide in human blood—What has been done and what is next? *Food Chem Toxicol*. 2022;112799.
- Sansano M, Heredia A, Peinado I, Andrés A. Dietary acrylamide: What happens during digestion. *Food chemistry*. 2017;237:58-64.
- Erdemli Z, Erdemli ME, Turkoz Y, Gul M, Yigitcan B, Gozukara Bag H. The effects of acrylamide and Vitamin E administration during pregnancy on adult rats testis. *Andrologia*. 2019;51(7):e13292.
- Michalak J, Czarnowska-Kujawska M, Klepacka J, Gujska E. Effect of microwave heating on the acrylamide formation in foods. *Molecules*. 2020;25(18):4140.
- Kucukler S, Caglayan C, Darendelioglu E, Kandemir FM. Morin attenuates acrylamide-induced testicular toxicity in rats by regulating the NF-κB, Bax/Bcl-2 and PI3K/Akt/mTOR signaling pathways. *Life Sci*. 2020;261:118301.
- Raffan S, Halford NG. Acrylamide in food: Progress in and prospects for genetic and agronomic solutions. *Ann Appl Biol*. 2019;175(3):259-81.
- Ledbetter M, Bartlett L, Fiore A, Montague G, Sturrock K, McNamara G. Acrylamide in industrial potato crisp manufacturing: a potential tool for its reduction. *LWT*. 2020;123:109111.
- Rahbardar MG, Farmad HC, Hosseinzadeh H, Mehri S. Protective effects of selenium on acrylamide-induced neurotoxicity and hepatotoxicity in rats. *Iran J Basic Med Sci*. 2021;24(8):1041.
- Tabeshpour J, Mehri S, Abnous K, Hosseinzadeh H. Neuroprotective effects of thymoquinone in acrylamide-induced peripheral nervous system toxicity through MAPKinase and apoptosis pathways in rat. *Neurochem Res*. 2019;44:1101-12.
- Gül M, Kayhan Kuştepe E, Erdemli ME, Altınöz E, Gözükara Bağ HG, Gül S, *et al.* Protective effects of crocin on acrylamide-induced testis damage. *Andrologia*. 2021;53(9):e14176.
- Kalaivani M, Saleena UV, Katapadi KGK, Kumar YP, Nayak D. Effect of acrylamide ingestion on reproductive organs of adult male wistar rats. *J Clin Diagnostic Res*. 2018;12(11).
- Besaratinia A, Pfeifer GP. A review of mechanisms of acrylamide carcinogenicity. *Carcinogenesis*. 2007;28(3):519-28.
- Aydin Y. Acrylamide and its metabolite glycidamide can affect antioxidant defenses and steroidogenesis in Leydig and Sertoli cells. *Toxicological & Environmental Chemistry*. 2018;100(2):247-57.
- Farag OM, Abd-Elsalam RM, El Badawy SA, Ogaly HA, Alsherbiny MA, Ahmed KA. Portulaca oleracea seeds' extract alleviates acrylamide-induced testicular dysfunction by promoting oxidative status and steroidogenic pathway in rats. *BMC Complement Altern Med*. 2021;21(1):1-15.
- Lebda M, Gad S, Gaafar H. Effects of lipoic acid on acrylamide induced testicular damage. *Materia socio-medica*. 2014;26(3):208-12.
- Sengul E, Gelen V, Yildirim S, Cinar İ, Aksu EH. Effects of naringin on oxidative stress, inflammation, some reproductive parameters, and apoptosis in acrylamide-induced testis toxicity in rat. *Environ Toxicol*. 2023;38(4):798-808.
- Katen AL, Sipilä P, Mitchell LA, Stanger SJ, Nixon B, Roman SD. Epididymal CYP2E1 plays a critical role in acrylamide-induced DNA damage in spermatozoa and paternally mediated embryonic resorptions. *Biol Reprod*. 2017;96(4):921-35.
- Trigg NA, Skerrett-Byrne DA, Xavier MJ, Zhou W, Anderson AL, Stanger SJ, *et al.* Acrylamide modulates the mouse epididymal proteome to drive alterations in the sperm small non-coding RNA profile and dysregulate embryo development. *Cell Reports*. 2021;37(1):109787.
- Zhang J, Zhu X, Xu W, Hu J, Shen Q, Zhu D, *et al.* Exposure to acrylamide inhibits testosterone production in mice testes and Leydig cells by activating ERK1/2 phosphorylation. *Food Chem Toxicol*. 2023;172:113576.
- Gervasi MG, Visconti PE. Molecular changes and signaling events occurring in spermatozoa during epididymal maturation. *Andrology*. 2017;5(2):204-18.
- Elbakry RH, Ibrahim MA. Histological, immunohistochemical and biochemical study of the effect of triclosan and its withdrawal on cauda epididymis of adult albino rat. *Egyptian Journal of Histology*. 2019;42(1):84-98.

24. Robaire B, Hinton BT, Orgebin-Crist M-C. The epididymis. Knobil and Neill's physiology of reproduction: Elsevier; 2006. p. 1071-148.
25. Ahmed MH, Sabry SM, Zaki SM, El-Sadik AO. Histological, immunohistochemical and ultrastructural study of the epididymis in the adult albino rat. *Aust J Basic Appl Sci.* 2009;3(3):2278-89.
26. Zhou W, De Iuliis GN, Dun MD, Nixon B. Characteristics of the epididymal luminal environment responsible for sperm maturation and storage. *Frontiers in Endocrinology.* 2018;9:59.
27. De Grava Kempinas W, Klinefelter GR. Interpreting histopathology in the epididymis. *Spermatogenesis.* 2014;4(2):e979114.
28. Leung G, Cheung K, Leung C, Tsang M, Wong P. Regulation of epididymal principal cell functions by basal cells: role of transient receptor potential (Trp) proteins and cyclooxygenase-1 (COX-1). *Mol Cell Endocrinol.* 2004;216(1-2):5-13.
29. Rinaldi VD, Donnard E, Gellatly K, Rasmussen M, Kucukural A, Yukselen O, *et al.* An atlas of cell types in the mouse epididymis and vas deferens. *elife.* 2020;9:e55474.
30. Shi J, Fok KL, Dai P, Qiao F, Zhang M, Liu H, *et al.* Spatio-temporal landscape of mouse epididymal cells and specific mitochondria-rich segments defined by large-scale single-cell RNA-seq. *Cell Discov.* 2021;7(1):34.
31. Leir S-H, Yin S, Kerschner JL, Cosme W, Harris A. An atlas of human proximal epididymis reveals cell-specific functions and distinct roles for CFTR. *Life Sci Alliance.* 2020;3(11):e202000744.
32. Caporali S, De Stefano A, Calabrese C, Giovannelli A, Pieri M, Savini I, *et al.* Anti-inflammatory and active biological properties of the plant-derived bioactive compounds luteolin and luteolin 7-glucoside. *Nutrients.* 2022;14(6):1155.
33. Cheng Y, Yang Z, Shi J, Yang J, Zhao J, He Y, *et al.* Total flavonoids of *Epimedium* ameliorates testicular damage in streptozotocin-induced diabetic rats by suppressing inflammation and oxidative stress. *Environ Toxicol.* 2020;35(2):268-76.
34. Mustafa S, Ijaz MU, ul Ain Q, Afsar T, Almajwal A, Shafique H, *et al.* Isorhamnetin: a flavonoid, attenuated doxorubicin-induced testicular injury via regulation of steroidogenic enzymes and apoptotic signaling gene expression in male rats. *Toxicol Res (Camb).* 2022;11(3):475-85.
35. Owumi SE, Ijделе AO, Arunsi UO, Odunola OA. Luteolin abates reproductive toxicity mediated by the oxido-inflammatory response in Doxorubicin-treated rats. *Toxicol Res Appl.* 2020;4:1-16.
36. Luo S, Li H, Mo Z, Lei J, Zhu L, Huang Y, *et al.* Connectivity map identifies luteolin as a treatment option of ischemic stroke by inhibiting MMP9 and activation of the PI3K/Akt signaling pathway. *Experimental & Molecular Medicine.* 2019;51(3):1-11.
37. Zhao L, Zheng M, Cai H, Chen J, Lin Y, Wang F, *et al.* The activity comparison of six dietary flavonoids identifies that luteolin inhibits 3T3-L1 adipocyte differentiation through reducing ROS generation. *The Journal of Nutritional Biochemistry.* 2023;112:109208.
38. Yahyazadeh A, Altunkaynak B. Protective effects of luteolin on rat testis following exposure to 900 MHz electromagnetic field. *Biotech Histochem.* 2019;94(4):298-307.
39. Struck MB, Andrutis KA, Ramirez HE, Battles AH. Effect of a short-term fast on ketamine-xylazine anesthesia in rats. *J Am Assoc Lab Anim Sci.* 2011;50(3):344-8.
40. Wu PY, Scarlata E, O'Flaherty C. Long-term adverse effects of oxidative stress on rat epididymis and spermatozoa. *Antioxidants.* 2020;9(2):170.
41. Katerji M, Filippova M, Duerksen-Hughes P. Approaches and methods to measure oxidative stress in clinical samples: Research applications in the cancer field. *Oxidative medicine and cellular longevity.* 2019;2019.
42. Weydert CJ, Cullen JJ. Measurement of superoxide dismutase, catalase and glutathione peroxidase in cultured cells and tissue. *Nature protocols.* 2010;5(1):51-66.
43. Bustin SA. Absolute quantification of mRNA using real-time reverse transcription polymerase chain reaction assays. *Journal of molecular endocrinology.* 2000;25(2):169-93.
44. Bancroft JD, Gamble M. *Theory and practice of histological techniques:* Elsevier health sciences; 2008.
45. Kuo J. *Electron microscopy: methods and protocols.* 3rd Ed. New Gersy: Humana press incorporation; 2014.
46. Solaiman AA, Nabil IM, Ramadan H, Eid AA. Histologic Study of the Possible Protective Effect of Resveratrol Versus Resveratrol-Loaded Niosomes Against Titanium Dioxide Nanoparticles-Induced Toxicity on Adult Rat Seminiferous Tubules. *Egyptian Journal of Histology.* 2020;43(4):1143-61.
47. Arun S, Burawat J, Sukhorum W, Sampannang A, Maneenin C, Iamsaard S. Chronic restraint stress induces sperm acrosome reaction and changes in testicular tyrosine phosphorylated proteins in rats. *Int J Reprod Biomed.* 2016;14(7):443.
48. Kirkpatrick LA, Feeny B. *A simple guide to IBM SPSS*

- statistics-version 20.0. student ed. Calif:Wadsworth: Cengage Learning; 2013.
49. Turner KA, Rambhatla A, Schon S, Agarwal A, Krawetz SA, Dupree JM, *et al.* Male infertility is a women's health issue—research and clinical evaluation of male infertility is needed. *Cells.* 2020;9(4):990.
 50. Ivanski F, de Oliveira VM, de Oliveira IM, de Araújo Ramos AT, de Oliveira Tonete ST, de Oliveira Hykavei G, *et al.* Prepubertal acrylamide exposure causes dose-response decreases in spermatic production and functionality with modulation of genes involved in the spermatogenesis in rats. *Toxicology.* 2020;436:152428.
 51. Di Nisio A, Foresta C. Water and soil pollution as determinant of water and food quality/contamination and its impact on male fertility. *Reprod Biol Endocrinol.* 2019;17:1-13.
 52. Friedman M. Chemistry, biochemistry, and safety of acrylamide. A review. *J Agric Food Chem.* 2003;51(16):4504-26.
 53. Al-Serwi RH, Ghoneim FM. The impact of vitamin E against acrylamide induced toxicity on skeletal muscles of adult male albino rat tongue: Light and electron microscopic study. *J Microsc Ultrastruct.* 2015;3(3):137-47.
 54. Cyr DG, Finnson K, Dufresne J, Gregory M. Cellular Interactions and the Blood-Epididymal Barrier. In: Robaire B, Hinton BT, editors. *The Epididymis: From Molecules to Clinical Practice: A Comprehensive Survey of the Efferent Ducts, the Epididymis and the Vas Deferens.* Boston, MA: Springer US; 2002. p. 103-18.
 55. Mori Y, Kobayashi H, Fujita Y, Yatagawa M, Kato S, Kawanishi S, *et al.* Mechanism of reactive oxygen species generation and oxidative DNA damage induced by acryloylhydroxamic acid, a putative metabolite of acrylamide. *Mutat Res Genet Toxicol Environ Mutagen.* 2022;873:503420.
 56. Jiang G, Zhang L, Wang H, Chen Q, Wu X, Yan X, *et al.* Protective effects of a Ganoderma atrum polysaccharide against acrylamide induced oxidative damage via a mitochondria mediated intrinsic apoptotic pathway in IEC-6 cells. *Food & function.* 2018;9(2):1133-43.
 57. Yilmaz BO, Yildizbayrak N, Aydin Y, Erkan M. Evidence of acrylamide-and glycidamide-induced oxidative stress and apoptosis in Leydig and Sertoli cells. *Human & experimental toxicology.* 2017;36(12):1225-35.
 58. Pan X, Wu X, Yan D, Peng C, Rao C, Yan H. Acrylamide-induced oxidative stress and inflammatory response are alleviated by N-acetylcysteine in PC12 cells: involvement of the crosstalk between Nrf2 and NF- κ B pathways regulated by MAPKs. *Toxicology letters.* 2018;288:55-64.
 59. Abd-Elsalam RM, El Badawy SA, Ogaly HA, Ibrahim FM, Farag OM, Ahmed KA. Eruca sativa seed extract modulates oxidative stress and apoptosis and up-regulates the expression of Bcl-2 and Bax genes in acrylamide-induced testicular dysfunction in rats. *Environ Sci Pollut Res.* 2021;28(38):53249-66.
 60. Iqbal A, Syed MA, Najmi AK, Ali J, Haque SE. Ameliorative effect of nerolidol on cyclophosphamide-induced gonadal toxicity in Swiss Albino mice: Biochemical-, histological-and immunohistochemical-based evidences. *Andrologia.* 2020;52(4):e13535.
 61. Bravo A, Quilaqueo N, Jofré I, Villegas JV. Overtime expression of plasma membrane and mitochondrial function markers associated with cell death in human spermatozoa exposed to nonphysiological levels of reactive oxygen species. *Andrologia.* 2021;53(2):e13907.
 62. Yang H-J, Lee S-H, Jin Y, Choi J-H, Han D-U, Chae C, *et al.* Toxicological effects of acrylamide on rat testicular gene expression profile. *Reproductive Toxicology.* 2005;19(4):527-34.
 63. Song H-X, Wang R, Geng Z-M, Cao S-X, Liu T-Z. Subchronic exposure to acrylamide affects reproduction and testis endocrine function of rats. *Zhonghua nan ke xue= National journal of andrology.* 2008;14(5):406-10.
 64. Pouretezari M, Talebi A, Abbasi A, Khalili MA, Mangoli E, Anvari M. Effects of acrylamide on sperm parameters, chromatin quality, and the level of blood testosterone in mice. *Int J Reprod Biomed.* 2014;12(5):335-42.
 65. O'Donnell L, Stanton P, de Kretser DM. *Endocrinology of the Male Reproductive System and Spermatogenesis:* MDText.com, Inc., South Dartmouth (MA); 2000.
 66. Ma Y, Shi J, Zheng M, Liu J, Tian S, He X, *et al.* Toxicological effects of acrylamide on the reproductive system of weaning male rats. *Toxicol Ind Health.* 2011;27(7):617-27.
 67. Camacho L, Latendresse J, Muskhelishvili L, Patton R, Bowyer J, Thomas M, *et al.* Effects of acrylamide exposure on serum hormones, gene expression, cell proliferation, and histopathology in male reproductive tissues of Fischer 344 rats. *Toxicol Lett.* 2012;211(2):135-43.
 68. Yildizbayrak N, Erkan M. Acrylamide disrupts the steroidogenic pathway in Leydig cells: possible mechanism of action. *Toxicological & Environmental Chemistry.* 2018;100(2):235-46.
 69. Mohamed M, Sulaiman SA, Jaafar H. Histological changes in male accessory reproductive organs in rats exposed to cigarette smoke and the protective effect of honey supplementation. *Afr J Tradit Complement Altern Med.* 2012;9(3):329-35.

-
70. de Andrade SF, Oliva SU, Klinefelter GR, De Grava Kempinas W. Epididymis-specific pathologic disorders in rats exposed to gossypol from weaning through puberty. *J Toxicol Pathol.* 2006;34(6):730-7.
 71. Pleuger C, Silva EJR, Pilatz A, Bhushan S, Meinhardt A. Differential immune response to infection and acute inflammation along the epididymis. *Frontiers in Immunology.* 2020;11:599594.
 72. Ijaz MU, Ayaz F, Mustafa S, Ashraf A, Albeshr MF, Riaz MN, *et al.* Toxic effect of polyethylene microplastic on testicles and ameliorative effect of luteolin in adult rats: Environmental challenge. *J King Saud Univ Sci.* 2022;34(4):102064.
 73. Xiao C, Xia M-L, Wang J, Zhou X-R, Lou Y-Y, Tang L-H, *et al.* Luteolin attenuates cardiac ischemia/reperfusion injury in diabetic rats by modulating Nrf2 antioxidative function. *Oxid Med Cell Longev.* 2019;2019.
 74. Tan X, Yang Y, Xu J, Zhang P, Deng R, Mao Y, *et al.* Luteolin exerts neuroprotection via modulation of the p62/Keap1/Nrf2 pathway in intracerebral hemorrhage. *Frontiers in Pharmacology.* 2020;10:1551.
 75. Tan L, Liang C, Wang Y, Jiang Y, Zeng S, Tan R. Pharmacodynamic effect of luteolin micelles on alleviating cerebral ischemia reperfusion injury. *Pharmaceutics.* 2018;10(4):248.
 76. Al-Megrin WA, Alkhuriji AF, Yousef AOS, Metwally DM, Habotta OA, Kassab RB, *et al.* Antagonistic efficacy of luteolin against lead acetate exposure-associated with hepatotoxicity is mediated via antioxidant, anti-inflammatory, and anti-apoptotic activities. *Antioxidants.* 2019;9(1):10.
 77. Wang H, Luo Y, Qiao T, Wu Z, Huang Z. Luteolin sensitizes the antitumor effect of cisplatin in drug-resistant ovarian cancer via induction of apoptosis and inhibition of cell migration and invasion. *J Ovarian Res.* 2018;11:1-12.
 78. Ma Q. Role of nrf2 in oxidative stress and toxicity. *Annu Rev Pharmacol Toxicol.* 2013;53:401-26.
 79. Zhan X, Li J, Zhou T. Targeting Nrf2-mediated oxidative stress response signaling pathways as new therapeutic strategy for pituitary adenomas. *Frontiers in Pharmacology.* 2021;12:565748.
 80. Li L, Sun H-y, Liu W, Zhao H-y, Shao M-l. Silymarin protects against acrylamide-induced neurotoxicity via Nrf2 signalling in PC12 cells. *Food Chem Toxicol.* 2017;102:93-101.
 81. Ma B, Zhang J, Zhu Z, Zhao A, Zhou Y, Ying H, *et al.* Luteolin ameliorates testis injury and blood-testis barrier disruption through the Nrf2 signaling pathway and by upregulating Cx43. *Molecular nutrition & food research.* 2019;63(10):1800843.
-

المخلص العربي

تقييم التأثير التخفيفي المحتمل للوتولين على السمية بوساطة الأكريلاميد على الخلايا لمبطنة للنسيج الطلائى لرأس البربخ في الجرذان البالغة: دراسة هستولوجية وكيميائية

إيمان محمد نبيل^١، بسمة عبد المنعم ماضي^٢، أماني عبد المنعم سليمان^١قسم الانسجة وبيولوجيا الخلايا،^٢ قسم التشريح الادمي وعلم الاجنة كلية الطب جامعة الاسكندرية

مقدمة: مؤخر، الأكريلاميد أحد المركبات الكيميائية المستخدمة في العديد من الصناعات، قد تم اكتشافه في الأغذية الغنية بالنشويات المتعرضة لدرجات حرارة عالية. ان الأكريلاميد يظهر هذه السمية من خلال توليد فواصل مؤكسدة. اللوتولين يعتبر فلافونويد قوي مضاد للأكسدة محتمل ان يخفف هذا التأثير السام.

الهدف من البحث: تقييم التغييرات الهستوكيميائية الناجمة عن الأكريلاميد على رأس البربخ في الجرذان البيضاء البالغة و الدور المحتمل للوتولين في تحسين هذه التغييرات.

طرق البحث: ٣٠ جرذاً بالغاً تم تخصيصهم في:

- المجموعة الأولى (المجموعة الضابطة) التي تناولت اما الماء المقطر (المجموعة المتفرعة الاولى) أو زيت الذرة (المجموعة المتفرعة الثانية).

- المجموعة الثانية استقبلت ١٠٠ ميليجرام/ كيلوجرام لوتولين يوميا عن طريق الفم.

- المجموعة الثالثة استقبلت ٦.٢٥ ميليجرام/ كيلوجرام اكريلاميد يوميا عن طريق الفم.

- المجموعة الرابعة تناولت مزيج من جرعات الاكريلاميد واللوتولين كما في المجموعة الثانية و الثالثة.

بعد ٢١ يوما تم ذبح الجرذان بعد ان تم وزنهم في بداية و نهاية التجربة. تم الحصول على الدم للكشف على مستوي هرمون التستوستيرون، كما تم تجميع السائل المنوي من ذيل البربخ لتحليل عدد الحيوانات المنوية وحركتها. وتم استخدام الأنسجة المتجانسة لقياس مستوى المألونديالداهيد و السوبر أوكسيد ديسميوتيز و التعبير الجيني لكلا من البروتين المرتبط اكس لعلامات الموت المبرمج للخلايا (باكس) و بي سي أل تو. كما تمت معالجة رؤوس البربخ و فحصها بالميكروسكوبات الضوئية و الالكترونية. و تم تعريض كل البيانات للتحليلات الاحصائية.

النتائج: الاكريلاميد أحدث خلافا في النسيج الطلائى لرأس البربخ مع توسع في المسافات ما بين الخلايا وفجوات و تغييرات في النواة و انخفاض في عدد و حركة الحيوانات المنوية و أوزان الحيوانات و التستوستيرون في الدم مع زيادة في مستوى المألونديالداهيد و انخفاض في السوبر أوكسيد ديسميوتيز. و ايضا ارتفاع ملحوظ للباكس مع انخفاض ملحوظ في البي سي أل تو. تناول مزيج من الاكريلاميد واللوتولين أدى الى التحسن في تركيب رأس البربخ و أوزان الحيوانات و مستوى التستوستيرون و السوبر أوكسيد ديسميوتيز و البي سي أل تو و عدد و حركة الحيوانات المنوية.

الاستنتاج: الاكريلاميد أحدث سمية هستوكيميائية في النسيج الطلائى لرأس البربخ و في نفس الوقت خفف اللوتولين من هذا التأثير.